EuroSun2026

ASSESSMENT OF HEAT PUMP INTEGRATION IN A LEGACY DISTRICT HEATING NETWORK IN CHILE

Cristóbal Doña, Francisco Fuentes, Diego Naranjo, Pablo Castillo, Camila Martin, Carlos Felbol
Fraunhofer Chile Research
cristobal.dona@fraunhofer.cl

Summary

This study assesses heat-pump integration in the district-heating network operated by COSSBO (*Comunidad de Servicios Remodelación San Borja*) in Santiago, Chile, using monthly domestic hot-water (DHW) records, reconstructed space-heating demand and an hourly thermo-hydraulic model. The base case supplies 4.884 GWh/year of useful heat from 7.346 GWh/year of plant generation. Modelled distribution losses represent 33.5%, mainly reflecting prolonged low-load operation; this estimate remains conditional on the equivalent pipe heat-transfer coefficient. Two reference heat-pump capacities of 1 and 5 MWth were assessed, together with a heat-pump capacity sweep from 0.25 to 5 MWth in 0.05 MWth increments. At an indicative electricity price of 115.63 EUR/MWh, neither the 1 nor the 5 MWth alternative reaches discounted payback within 28 years. Under the estimated avoided-biomass operation and maintenance (O&M) assumption, only sub-MW capacities at hypothetical all-in electricity prices of 60–69 EUR/MWh yield positive NPVs; no tested capacity remains profitable when only half of that uncertain saving is realised. The findings support further assessment of staged base-load electrification, conditional on verified operating savings, electricity-contract access and an adequate waste-heat source.

Keywords: District heating, heat pump, retrofit, legacy network, techno-economic assessment, thermo-hydraulic simulation

Field of application for the findings: Sustainable and Efficient Districts: Innovative District Heating and Cooling, Urban Planning of Districts, Simulations, Digitalization and AI

Addressed audience: District heating researchers, utility and municipal planners, heat pump integrators, and decision-makers involved in the decarbonisation of existing urban energy systems

1. Introduction

Large-scale heat pumps are increasingly seen as an effective way to decarbonise district heating (DH) because they can integrate renewable and recovered heat sources (David et al., 2017; Sayegh et al., 2018). However, retrofitting older networks can be difficult, since many operate at high temperatures, are oversized for current demand, and suffer significant heat losses due to ageing infrastructure (Averfalk et al., 2017; Lund et al., 2014). Chile offers a relevant context where large-scale DH remains uncommon, and the COSSBO system in Santiago constitutes a unique tunnel-based urban network, supplying space heating and domestic hot water (DHW) to roughly 3,000 apartments through 26 buildings and 19 substations, currently dominated by biomass-based generation. As with many legacy assets, retrofit assessment is challenged by incomplete substation-level metering, limited temperature monitoring along the primary network, and the need to reconcile fuel-based production data with delivered heat, uncertainties that become critical when evaluating electrification under local electricity tariffs and capital constraints. Against this backdrop, this study reconstructs 2024 system operation and assesses the pre-feasibility of integrating a central heat pump under a favourable waste-heat-source scenario by combining reconstructed demand profiles, thermo-hydraulic network modelling, and an incremental techno-economic framework to quantify the impact of distribution losses and compare alternative heat pump sizing strategies, with the goal of clarifying the structural conditions under which electrification of legacy DH systems becomes technically and economically viable.

2. Case study and data

COSSBO operates a central thermal plant and a tunnel-based district-heating network serving the Remodelación San Borja residential complex in the commune of Santiago, Chile (Figure 1). Heat is supplied primarily by a 3 MW biomass boiler using hazelnut shells, with additional biomass-capable and gas-fired backup units. A plate heat exchanger separates the generator circuit from the primary network, which supplies the buildings through heat-transfer substations. Secondary systems, including storage-tank controls typically set at 50–55 °C, were excluded from the model (COSSBO, 2024). The assessment therefore covers the central plant, the primary supply and return network, and heat transfer at each substation. The principal system characteristics and modelling boundaries are summarised in Table 1.

The network was designed for a larger connected load than it currently serves, resulting in comparatively large pipe diameters and low present-day flow rates. Its ageing infrastructure, low-cost biomass baseline and documented operating history make it a relevant case for assessing heat-pump integration in an existing district-heating system.

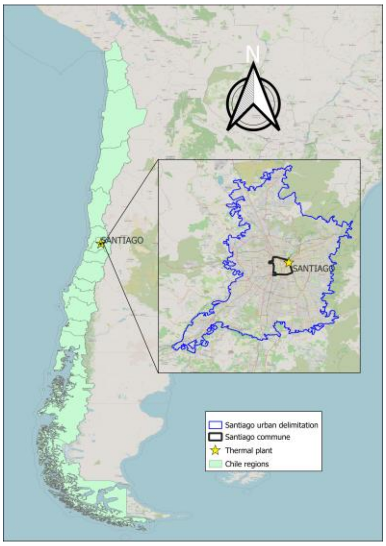

Figure 1 Location of the COSSBO district-heating system in Santiago Centro, Chile.

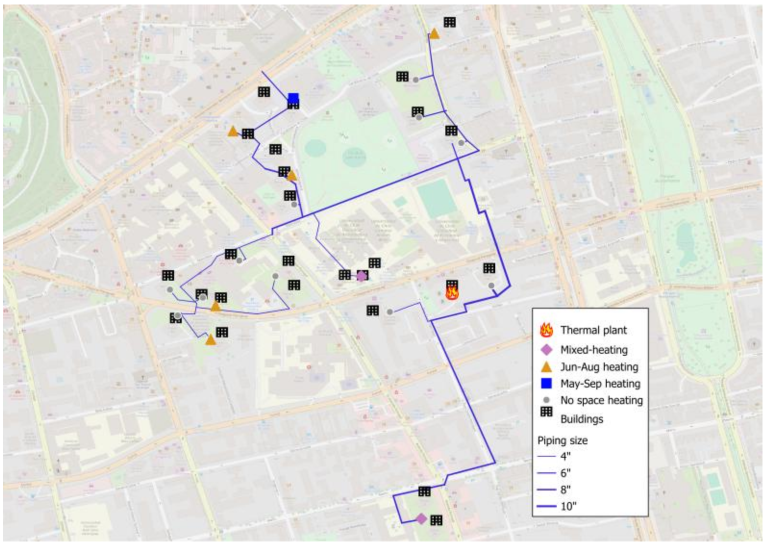

Figure 2 Layout of the COSSBO district-heating network and space-heating service periods. Mixed substations supply buildings with different seasonal schedules.

The evidence base comprised operator records, engineering documentation, site observations and previous measurement campaigns (COSSBO, 2024). Building-level DHW billing data were available for 2022–2024, whereas space-heating demand was reconstructed from commercial records, documented service periods and measurements from Torre 6. Plant logbooks provided daily operating variables, while higher-resolution supervisory control and data acquisition (SCADA) records were incomplete. Network geometry and pipe diameters were obtained from engineering drawings.

Table 1 Case-study characteristics and analysis boundary

Item	Description
Service	Domestic hot water and space heating
District-heating system	COSSBO central plant and legacy tunnel-based primary network
Buildings/substations	26/19
Primary network length	3.13 km
Primary supply temperature	67.8-79°C
Existing heat supply	3 MW main biomass boiler; additional biomass-capable and gas-fired backup units
Network representation	Supply and return pipes, substations and explicit bypasses
Outside boundary	Generator-side dynamics, secondary circuits, storage tanks and apartment controls, waste-heat source identification and source-side assessment

Primary supply and return temperatures indicate a temperature difference of approximately 5–15 °C across summer and winter operating conditions. Return temperatures remain relatively stable at around 63–65 °C, while supply temperatures vary between approximately 70 and 78 °C to accommodate seasonal changes in heat demand. Because these noon observations do not represent the full diurnal or annual distribution, they are used as plausibility checks rather than direct hourly calibration targets, and monthly supply-temperature setpoints are explicitly imputed where reliable data are unavailable. Throughout the analysis, inputs are therefore clearly classified as measured, reconstructed, or assumed, as summarised in Table 2.

Table 2 Evidence base and role in the analysis

Evidence stream	Main source	Variable or purpose
Domestic-hot-water consumption	Building-level DHW records	Monthly volume $[m^3]$ by building
Space-heating demand	Torre 6 heat-measurement case and reference profiles	Heating-to-DHW relationship; identification of heating-connected buildings and service periods
Plant operating log	Thermal plant summary 2024	Gas/electricity readings, pressure, pump state, primary supply/return temperature
Fuel procurement	Biomass and gas records	Fuel mass, fuel cost and plant energy estimate
Flow campaign	Central-plant and remote-substation flow report	Flow and temperature consistency check
Network geometry	Drawings and geographic information system (GIS) reconstruction	Pipe topology, length and diameter
Heat-pump performance	Technology guideline and supplier/planning assumption	Seasonal coefficient of performance (SCOP) and investment-cost range

3. Methodology

3.1 Demand reconstruction and hourly profiles

Building demand was combined with a QGIS reconstruction of the primary network (Figure 2) to generate hourly boundary conditions for pandapipes and subsequent heat-pump assessment (QGIS Development Team, 2026).

Reported 2024 monthly DHW volumes were converted to useful heat using (eq. 1), with a representative temperature rise of 35 K between cold water at approximately 15 °C and delivered DHW at 50 °C, as reviewed with COSSBO. Each building's reported monthly DHW energy was preserved.

$$Q_{DHW} = V_{DHW} \rho c_p \Delta T \qquad \text{(eq. 1)}$$

Space heating was billed by building and service season rather than by metered energy. Annual heating targets were therefore derived from the original DHW-based reconstruction over each building's documented service period. Its effective heating-to-DHW multiplier was approximately 3.56, corresponding to a 78% heating share at the reference stage, broadly consistent with an unpublished measurement study in one connected building (COSSBO, 2024). These annual targets were retained while DHW was independently reconciled with monthly billing records; consequently, the final profiles do not impose a fixed daily or monthly heating-to-DHW ratio. Heating for two buildings without usable DHW records was imputed from comparable connected buildings.

Separate normalised weekday and weekend templates shown in Figure 3 represent DHW morning/evening peaks and a broader heating schedule (Braas et al., 2020; Weissmann et al., 2017). A normalised calendar envelope centred on mid-winter allocates annual heating within each service period. It is a simplified seasonal assumption, rather than a weather-dependent model (Ruhnau et al., 2019). An assumed weekend weighting of 1.08 redistributes energy within the prescribed totals. A one-hour shift in one building reduces peak coincidence without changing energy; the resulting 5–6 MW peak agreement is therefore a plausibility constraint, not independent validation. Total reconstructed useful demand is 4.888 GWh/year.

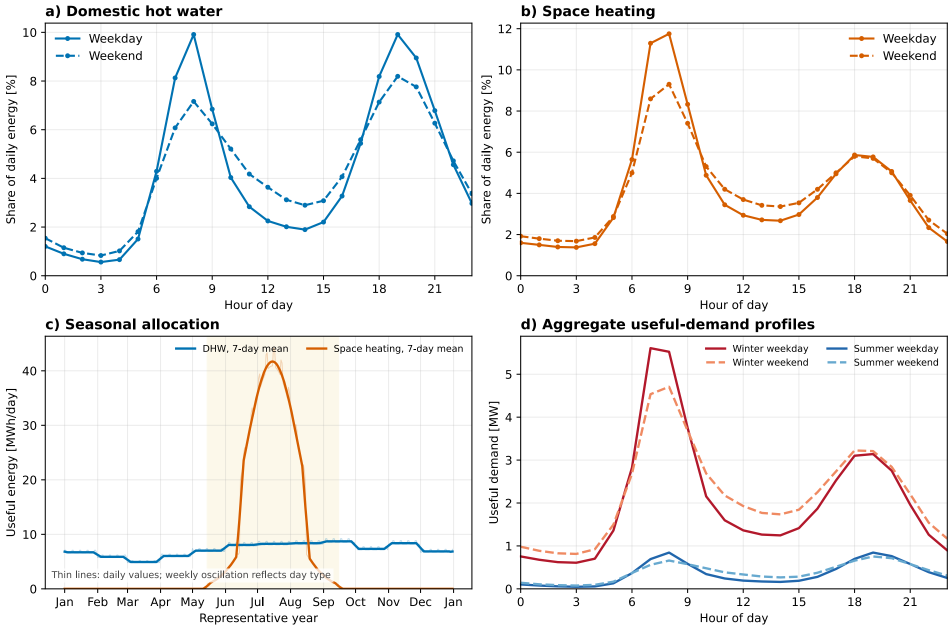

Figure 3 Synthetic DHW and heating demand: (a–b) normalised weekday/weekend templates; (c) monthly service energies; (d) representative winter/summer daily profiles. DHW monthly totals follow billing records; heating seasonality is assumed.

Fuel-based annual heat production was estimated from recorded fuel quantities, lower heating values and an assumed boiler efficiency of 91%. Relative to this estimate, reconstructed useful demand leaves an unresolved residual of approximately 57%. Possible contributors include fuel-stock and reporting-period mismatches, uncertain biomass moisture and calorific value, actual seasonal boiler efficiency, unmetered heat uses, losses outside the primary-network boundary and uncertainty in reconstructed heating demand. Their individual contributions cannot be separated with the available records. The residual is therefore an accounting gap, not a measured distribution-loss fraction; primary-network losses were estimated independently by the thermo-hydraulic model.

3.2 Thermo-hydraulic network model

The primary network is modelled with pandapipes, an open-source steady-state pipe-flow library that couples hydraulic and thermal calculations (Lohmeier et al., 2020). Each hour is solved as an independent quasi-steady state. Supply and return circuits are represented explicitly, pipe lengths and diameters are inherited from the GIS network, and long pipes are thermally discretised into sections no longer than 10 m. This discretisation reduces the thermal overshoot observed when a long, low-flow pipe is treated as a single control volume.

Pipe heat transfer is represented through an equivalent overall coefficient U applied to the internal surface used by pandapipes. For a section of internal diameter D_i, where T_{amb} is the ambient temperature and T_{water} water temperature, the corresponding steady heat exchange is expressed in (eq. 2).

$$Q_{loss} = U\pi D_i L(T_{water} - T_{amb}) \qquad \text{(eq. 2)}$$

A constant U = 2 W/(m²K) is retained as the base-case equivalent because the network combines old pipes, uncertain insulation condition and tunnel exposure. It is not presented as a measured material property. Reported values for district-heating networks span a broad range depending on insulation, diameter, age, moisture and installation (Chicherin et al., 2020; IEA District Heating and Cooling Programme, 2008; Jakubek et al., 2023); the sensitivity U = 1–3 W/(m²K) therefore carries more information than the point estimate. Future calibration should assign U by pipe class and condition rather than forcing a constant linear loss. The complete base-case parameter set is reported in Table 3.

Table 3 Thermo-hydraulic model parameters

Parameter	Value used in base case	Interpretation
Working fluid	Water	–
Supply-temperature setpoint	Monthly 67.8–79.0 °C	Based on available plant records; missing months imputed
Ambient tunnel temperature	20 °C	Uniform provisional value; tested at 15 and 25 °C
Design temperature difference at substations	20 K	Substation design target, not an imposed operating ΔT
Minimum valid return	30 °C	Controller constraint, not a calibrated return setpoint
Minimum total circulation	10 kg/s	Provided through four provisional terminal bypasses
Local bypass	0.005 kg/s/substation when off	Prevents fully stagnant local branches
Plant reference pressure	3.0 bar	
Pump pressure lift	1.0 bar	
Pipe roughness	0.15 mm	Hydraulic assumptions
Minor-loss coefficient	0.10	Hydraulic assumptions
Equivalent overall heat-transfer coefficient U	2.0 W m-2 K-1	Uniform provisional value; tested at 1 and 3
Water specific heat	4.180 kJ kg-1 K-1	Thermal assumptions

3.3 Physical substation controller and consistency check

The load-side control strategy is designed to satisfy the requested heat demand while respecting hydraulic and thermal operating limits. The design temperature difference of 20 K is used only to define the preferred mass flow through each load. Actual heat delivery Q_{del} is determined by the available supply temperature and the physically admissible flow rate. As expressed in Eqs. (3)-(5), the delivered heat cannot exceed either the requested demand Q_{dem} or the thermal energy that can be extracted from the available flow while maintaining the prescribed minimum return temperature. Any difference between the requested and delivered heat is recorded as unmet demand Q_{unmet}.

$$Q_{del} \leq Q_{dem} \qquad \text{(eq. 3)}$$

$$Q_{del} \leq \dot{\mathrm{m}}_{\mathrm{load}} c_p (T_{supply} - T_{return,min}) \qquad \text{(eq. 4)}$$

$$Q_{unmet} = Q_{dem} - Q_{del} \geq 0 \qquad \text{(eq. 5)}$$

The load path at each substation consists of a heat exchanger and a passive control valve. The valve coefficient is iteratively adjusted so that the resulting thermo-hydraulic state approaches the required load flow while maintaining a positive pressure drop across the substation. If the available temperature difference is insufficient to meet the heat demand at the preferred flow, the controller increases the flow up to a predefined maximum value. If the requested heat still cannot be supplied without violating the minimum return-temperature constraint, heat delivery is reduced accordingly and the remaining demand is classified as unmet heat, consistent with (eq. 5).

Each hourly simulation is treated as an independent steady-state calculation. Consequently, valve coefficients are reset before solving each hour. This prevents the numerical state obtained in one timestep from influencing the solution of the following timestep and ensures that the result for a given hour does not depend on its position within the annual simulation sequence. The procedure therefore avoids artificial path dependence without introducing dynamic behaviour that is not explicitly represented in the model.

Network circulation is treated separately from consumer heat delivery. When a substation has no thermal demand, a small local bypass maintains circulation through the corresponding branch. In addition, terminal bypasses located at four remote branches maintain a provisional network-wide minimum circulation of 10 kg/s. These bypasses progressively close as consumer flow increases. The resulting return temperature is calculated from an energy balance that accounts for the mixing of consumer and bypass flows. Maintaining bypass circulation can support adequate supply temperatures at remote parts of the network and increase the mixed return temperature, although it also leads to greater pipe heat losses and pumping requirements. The assumed bypass locations and minimum circulation rate should therefore be verified against the actual network operating strategy.

Finally, every hourly solution is subjected to a set of numerical and physical consistency checks. These include finite temperatures, pressures, and mass flows; physically valid supply and return temperatures; non-negative delivered and unmet heat; energy balance closure at each substation; positive passive pressure losses; and solver convergence.

3.4 Heat-pump dispatch and economic assessment

Heat-pump integration was assessed conditionally because no waste-heat source has yet been characterised. The condenser was assumed to heat the primary return to the monthly 67.8–79.0 °C supply setpoint, in parallel with the existing plant heat exchanger; biomass supplies residual demand and backup. SCOP = 4.4 was adopted from the German technology catalogue as a favourable performance assumption (Kompetenzzentrum Kommunale Wärmewende (KWW), 2024). Source-side feasibility was checked approximately using a Carnot-based COP estimate, a second-law efficiency of 0.5 and assumed 5 K heat-exchanger approaches (Averfalk et al., 2021). Achieving COP ≈ 4.4 would then require source-water inlet temperatures of approximately 48 °C at the mean network supply temperature and 53 °C at the maximum setpoint. These indicative requirements do not establish source availability or validate annual SCOP. The 1 and 5 MWth alternatives represent base-load and near-full-load integration; intermediate capacities were subsequently screened using the same hourly plant load and (eq. 9).

Economic feasibility was evaluated using an incremental retrofit approach, considering only costs and savings directly attributable to heat-pump integration. Capital expenditure (CAPEX) and fixed operation and maintenance costs (O&M) were derived from European prefeasibility cost data (Kompetenzzentrum Kommunale Wärmewende (KWW), 2024) and were not adjusted to Chile-specific equipment, labour, logistics, or electrical-interconnection costs. Catalogue investment costs were interpreted as EUR 2022 values and converted to EUR 2024 using a factor of 1.0793. An indicative free-customer electricity benchmark was derived from the Chilean National Energy Commission's market-price indicator, while the biomass price was obtained from COSSBO fuel records. Both were expressed using the project's 2024 currency-conversion assumptions, resulting in 115.6 €/MWh for electricity and 21.13 €/MWh for biomass fuel (Comisión Nacional de Energía, 2026; COSSBO, 2024). Boiler efficiency was assumed to be 91%, and heat-pump fixed O&M was set at 2.5% of CAPEX per year. Hourly heat-pump generation was used to determine electricity consumption and displaced biomass generation, from which annual incremental operating savings were calculated.

Undocumented biomass-boiler O&M was estimated from Danish fixed and variable cost data (Danish Energy Agency, 2016) and treated as a screening proxy rather than audited COSSBO expenditure. The reported 3 MW main biomass boiler was used as the capacity basis: applying a fixed-O&M coefficient of 32,500 EUR/(MWth·year) gives $F = 97{,}500$ EUR/year. Non-energy variable O&M was set at $v = 1.19$ EUR/MWh. The source-year values were retained without escalation and treated as approximate EUR 2024 screening inputs, with their uncertainty addressed through the avoided-O&M sensitivity analysis. Because the biomass plant remains available for residual heat supply and backup, its O&M was not assumed to be fully avoided. As expressed in Equations (6)-(8), retained boiler O&M consists of a 20% fixed standby component, a further 80% of fixed expenditure scaled according to the residual biomass heat share, and variable O&M proportional to residual biomass generation. Here, F is reference annual fixed boiler O&M, v is the non-energy variable O&M coefficient, E_{plant} is annual simulated plant heat generation before heat-pump dispatch, and E_{bio} is annual heat remaining to be supplied by biomass. Avoided boiler O&M is calculated as the difference between the reference and retained costs. Scaling part of fixed expenditure with thermal output is a screening assumption about avoidable operating activity rather than an observed cost response; the 20% standby floor was likewise assumed rather than measured.

$$C_{boiler,ref} = F + vE_{plant} \quad \text{(eq. 6)}$$

$$C_{boiler,retained} = F\left[0.2 + 0.8\frac{E_{\mathrm{bio}}}{E_{\mathrm{plant}}}\right] + vE_{bio} \quad \text{(eq. 7)}$$

$$C_{boiler,avoided} = C_{boiler,ref} - C_{boiler,retained} \quad \text{(eq. 8)}$$

Annual cash flow equals avoided fuel and boiler O&M expenditure minus heat-pump electricity and fixed O&M costs. NPV and discounted payback were calculated over 28 years at a 5% real discount rate, assuming constant annual performance and real costs, without replacement or residual value. Pumping electricity and source-specific integration costs were not separately quantified. The existing distribution network is common to both alternatives and was treated as a sunk asset. Equations (9)–(11) describe dispatch, CAPEX and NPV; in (eq. 10), capacity is in MWth, α = 1210.6, b = −0.28 and the EUR 2022-to-2024 factor is 1.0793. Discounted payback is the first year with non-negative cumulative discounted cash flow.

$$\dot{Q}_{HP,t} = \min(\dot{Q}_{plant,t}, P_{HP}),\ \dot{Q}_{boiler,t} = \dot{Q}_{plant,t} - \dot{Q}_{HP,t} \quad \text{(eq. 9)}$$

$$\mathrm{CAPEX_{HP}} = 1000\mathrm{P_{HP}}\mathrm{F}_{2022\rightarrow 2024}\alpha P_{HP}^{b} \quad \text{(eq. 10)}$$

$$\mathrm{NPV} = -\mathrm{CAPEX} + \sum_{y=1}^{28}\frac{CF_y}{(1+r)^y} \quad \text{(eq. 11)}$$

3.5 Sensitivity analysis

One-at-a-time physical sensitivity varied U = 1–3 W/(m²K), ambient temperature = 15–25 °C, minimum circulation = 5–15 kg/s and design temperature difference = 15–25 K around the base case. Economic sensitivity used the physical base load: CAPEX and biomass price ±10% and ±20%, discount rate ±2 percentage points, and heat-pump fixed O&M of 1.5–3.5% of CAPEX/year. Electricity scenarios comprised hypothetical all-in power purchase agreement (PPA) prices of 60, 69 and 78 EUR/MWh, the 115.63 EUR/MWh benchmark and the current-price counterfactual of 159.6 EUR/MWh. SCOP was held constant because electricity expenditure depends on the ratio of electricity price to SCOP. Additional robustness checks varied realised avoided biomass O&M from 0% to 150% of its current estimate and screened capacities of 0.25–5 MWth in 0.05 MWth increments, including no investment. For each capacity, dispatch and economic costs were recalculated with (eq. 9); 0%, 50%, 100% and 150% avoided-O&M cases were examined as a postprocessing stage.

4. Results

4.1 Base-case thermo-hydraulic performance

The base simulation delivers 4.884 of the reconstructed 4.888 GWh/year useful demand, corresponding to 99.92% demand satisfaction. Plant generation reaches 7.346 GWh/year, including 2.462 GWh/year of modelled distribution heat loss, equivalent to 33.51% of plant generation. Peak useful demand is 5.608 MW, while simultaneous plant output reaches 5.734 MW, within the historically reported 5–6 MW range. The remaining thermo-hydraulic indicators are summarised in Table 4.

All 8,760 hourly states were solved and classified as physically valid. The iterative controller generated 35 tolerance warnings across 34 hours, but the hydraulic and thermal solvers converged and all mass, pressure and energy checks remained valid. Unmet heat is spatially concentrated: substation 73 accounts for approximately 3.73 MWh of the annual 3.79 MWh/year. This points to a local hydraulic or parameterisation issue rather than a system-wide inability to supply the reconstructed demand.

Table 4 Base case main simulation results

Metric	Base-case result
Useful demand / delivered heat	4.888 / 4.884 GWh/year
Unmet heat / demand supplied	3.79 MWh/year / 99.9%
Plant generation	7.35 GWh/year
Distribution thermal loss	2.46 GWh/year (33.5% of plant generation)
Peak / delivered / unmet demand	5.6 / 5.45 / 0.16 MW
Simultaneous plant output / pipe loss	5.73 / 0.29 MW
Plant supply temperature	Mean 73.2 °C; range 67.8–79.0 °C
Plant return temperature	Mean 58.1 °C; P05–P95 50.7–66.4 °C; minimum 44.2 °C
Mean plant temperature difference	15 K
Plant mass flow	Mean 12.4 kg/s; P95 26.1 kg/s; maximum 59.1 kg/s
Pressure range / maximum pipe velocity	2.0–3.0 bar / 1.47 m/s

The winter design condition provides the clearest spatial summary of the model, as shown in Figure 4. At the peak hour, supply temperatures at active substations range approximately from 71.9 to 77.7 °C. Supply pressure decreases from the 3 bar plant boundary to approximately 2.5 bar at the most hydraulically remote locations, while the maximum pipe velocity reaches 1.471 m/s. Low velocities in some branches reflect the large legacy pipe diameters relative to current local loads rather than an absence of pressure loss.

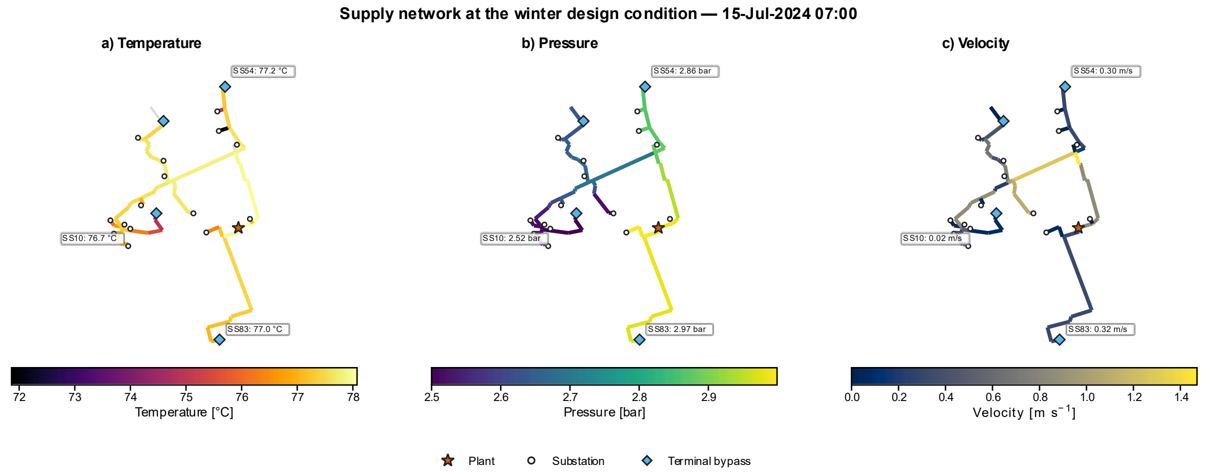

Figure 4 Supply-network temperature, pressure and velocity at the winter design condition

The monthly supply setpoint and the activation of space heating during the building-specific heating periods between mid-May and mid-September produce the clear seasonal operating pattern shown in Figure 5. During the winter peak, the plant supplies 5.734 MW at 57.12 kg/s; at the representative summer peak, it supplies 0.909 MW at 10.40 kg/s. The corresponding instantaneous loss fractions are 5.0% and 26.7%, respectively. The high summer fraction does not imply greater absolute heat loss at that hour; it results from maintaining a warm network while useful demand is small.

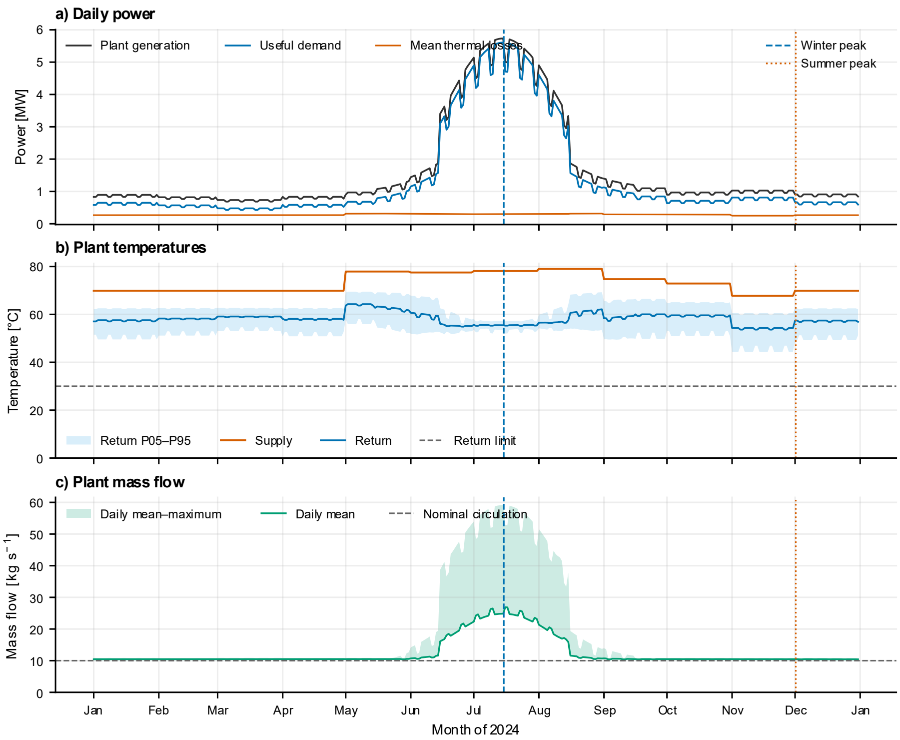

Figure 5 Daily plant generation, useful demand, thermal losses, primary temperatures and plant mass flow for the base case

4.2 Physical sensitivity

U dominates physical sensitivity: increasing it from 1 to 3 W/(m²K) raises annual thermal losses from 1.279 to 3.556 GWh and their share from 20.75% to 42.14%. Varying ambient temperature from 15 to 25 °C reduces losses from 2.717 to 2.207 GWh. Increasing minimum circulation from 5 to 15 kg/s improves low-load return temperatures but raises losses from 2.237 to 2.561 GWh, with negligible change in unmet heat. Reducing design ΔT from 20 to 15 K increases flow P95 from 26.13 to 35.30 kg/s and unmet heat from 3.79 to 11.83 MWh; increasing it to 25 K reduces these to 21.16 kg/s and 0.76 MWh.

4.3 Heat-pump dispatch and economic performance

The 1 MWth alternative supplies 77.69% of plant heat over 5,707 equivalent full-load hours. Increasing capacity to 5 MWth adds only 1.617 GWh/year of biomass displacement while increasing CAPEX by 2.856 M€. At 115.63 EUR/MWh, the 1 MWth case produces a positive annual cash flow of 17.28 k€/year but an NPV of −1.049 M€, whereas the 5 MWth case produces −39.97 k€/year and an NPV of −4.758 M€. Neither reaches discounted payback within 28 years (Table 5).

At 1 MWth, NPV ranges from −1.899 M€ at 159.61 EUR/MWh to +0.026 M€ at 60 EUR/MWh. Only the 60 EUR/MWh case reaches discounted payback, in year 27, and it requires approximately 97% of the estimated avoided-O&M saving to break even. The 69 and 78 EUR/MWh cases remain negative at −0.148 and −0.322 M€, respectively, while the 5 MWth alternative remains negative at every tested electricity price.

Table 5 Economic parameters for the 1 MWth and 5 MWth Heat Pump cases

Metric	1 MWth Heat Pump	5 MWth Heat Pump
CAPEX	1.307 M€	4.163 M€
Heat-pump heat	5.707 GWh/year	7.324 GWh/year
Share of plant heat	77.69%	99.71%
Equivalent full-load hours	5,707 h/year	1,465 h/year
Electricity use	1.297 GWh/year	1.665 GWh/year
Estimated avoided biomass O&M	67.39 k€/year	86.49 k€/year
Net annual cash flow	+17.28 k€/year	−39.97 k€/year
NPV, 28 years at 5%	−1.049 M€	−4.758 M€
Discounted payback	Not reached	Not reached

Capacity screening yields maximum NPVs of +0.214 M€ at 0.60 MWth and 60 EUR/MWh and +0.082 M€ at 0.50 MWth and 69 EUR/MWh. At 78 and 115.63 EUR/MWh, the no-investment outperforms all non-zero heat-pump capacities tested. If only 50% of the estimated avoided biomass O&M is realised, no capacity achieves a positive NPV, including at 60 EUR/MWh. Figure 6 summarises the combined effects of capacity, tariff, avoided O&M and the remaining sensitivities.

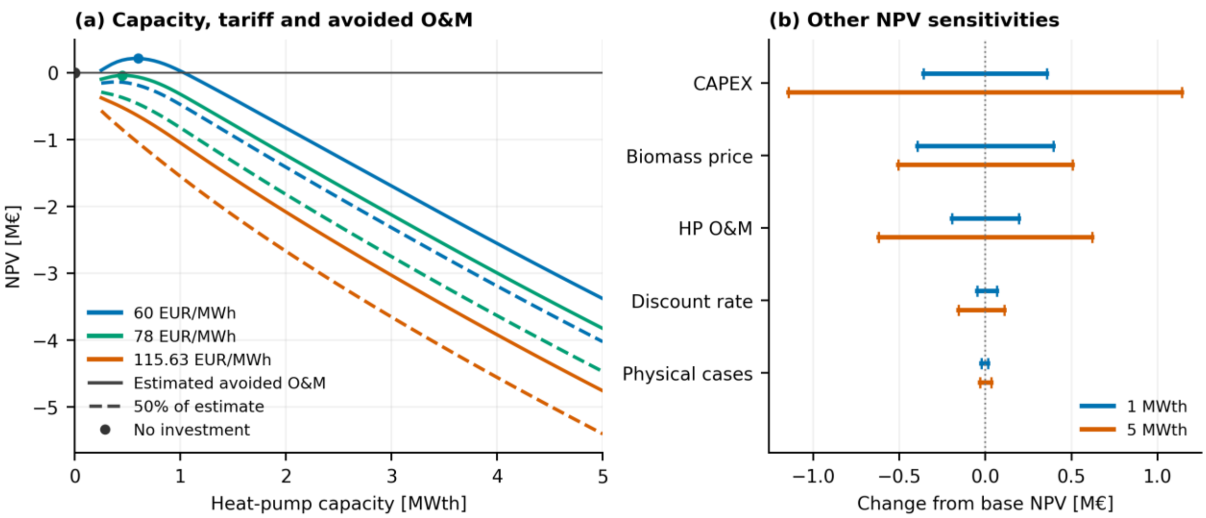

Figure 6 Economic robustness: (a) capacity screening at three all-in electricity prices, with 100% (solid) and 50% (dashed) of estimated avoided biomass O&M; (b) other NPV sensitivities at 115.63 EUR/MWh. Coloured markers identify the best sampled capacities under full estimated savings; the black marker denotes no investment. PPA prices are hypothetical. Monetary values are expressed in EUR 2024.

5. Discussion

The high annual loss fraction reflects the energy required to maintain a long, warm network during low-load operation. Average thermal loss is approximately 0.281 MW, close to 0.288 MW at the winter peak, while useful demand varies strongly. However, the 33.5% result is conditional on U = 2 W/(m²K), and the 20.75–42.14% sensitivity range precludes treating it as a measured network property. Pipe-condition surveys and synchronised heat metering are needed before detailed retrofit design; higher circulation also trades improved low-load temperatures against greater standing losses.

Monthly DHW closure improves consistency with billing records, but heating magnitude and timing remain reconstructed from one building study, transferred assumptions and synthetic profiles. The calendar envelope and imposed diversity therefore affect peak timing and capacity screening without independently validating hourly demand. Fragmented manual and SCADA records also prevent reconciliation of the fuel-based balance: its 57% residual may include accounting mismatches, uncertain conversion efficiency, unmetered uses and losses outside the primary-network boundary. Measurement priorities are plant heat output, representative building heat delivery and the local restriction at substation 73, which concentrates most simulated unmet heat.

A representative Carnot-based check indicates source-water inlet temperatures of approximately 48–53 °C to support COP ≈ 4.4 over the adopted network supply range, assuming 50% of Carnot performance, 5 K approaches at both heat exchangers and 5 K source cooling. This is an indicative source requirement, not evidence of an available resource or validation of annual SCOP. At COP = 4.4, full-load source extraction would be approximately 0.77 MW for the 1 MWth option and 3.86 MW for 5 MWth. Temperature, recoverable capacity and availability must therefore be verified jointly.

Tariff access and genuinely avoidable expenditure jointly control investment viability. Scaling the Danish fixed-O&M coefficient to the reported 3 MW main biomass boiler materially weakens the economic case: only a narrow sub-MW range remains positive at 60–69 EUR/MWh when the full estimated saving is realised, and none remains positive when that saving is halved. The 20% standby floor does not represent an observed COSSBO cost response; personnel, compliance, fuel-handling readiness and scheduled maintenance may remain even at low biomass generation. Local accounts and a defined backup operating strategy are therefore required before avoided O&M can be credited in an investment decision.

Although investment performance is more sensitive to electricity price, CAPEX and avoided biomass O&M than to the individual physical parameters tested, the hourly network model remains essential for translating useful demand into plant-side generation and determining heat-pump dispatch, equivalent full-load hours, biomass displacement and technically suitable capacity. The physical and economic analyses therefore fulfil complementary roles: economic assumptions determine whether electrification is attractive, whereas network simulation determines what can realistically be installed and operated. In particular, the load-duration curve shows why a smaller base-load unit can achieve substantially greater utilisation than a near-full-load alternative.

Future work should first calibrate primary flow, return temperature, heat delivery and pipe losses using synchronised measurements, while improving the reconstruction of building heating demand. The economic assessment should likewise be refined using Chilean supplier quotations, locally applicable heat-pump installation costs, electricity-contract conditions and audited biomass operation and maintenance expenditure, instead of relying primarily on adapted European cost references. Subsequent model development could replace the constant SCOP and tunnel temperature with hourly source- and ambient-temperature profiles, allowing heat-pump performance and network losses to vary temporally. If sufficient operational data become available, secondary storage, thermostat hysteresis and heat-exchanger controls could also be represented dynamically. These extensions would improve source sizing, return-temperature prediction and investment assessment, but should follow rather than replace the immediate measurement and calibration effort.

Consequently, staged base-load electrification warrants further assessment, whereas the 5 MWth alternative remains unattractive across the tested tariff and O&M ranges. Pumping electricity, detailed source-integration costs and lifecycle emissions remain outside the quantified assessment; the results therefore indicate conditional economic potential rather than a demonstrated investment or decarbonisation benefit.

6. Conclusions

COSSBO is an important Chilean reference case, combining an ageing tunnel-based network, large legacy pipes and reduced present-day load. Records, operator observations and low simulated velocities indicate partial oversizing. Investment should therefore prioritise metering, pipe-condition assessment, targeted loss reduction and operational optimisation rather than large-scale biomass replacement. Reconnecting buildings or adding year-round consumers could improve infrastructure utilisation and reduce the relative importance of standing losses, subject to available capacity.

The hourly model supplies 4.884 of 4.888 GWh/year of reconstructed useful demand, with plant generation of 7.346 GWh/year and a peak of 5.734 MW. The simulated 33.5% thermal-loss fraction mainly reflects the continuous operation of a long, warm network during prolonged low-load periods and remains conditional on equivalent pipe heat transfer; varying U from 1 to 3 W/(m^{2}K) changes this fraction from 20.75% to 42.14%.

Monthly DHW balances are constrained by records, whereas heating demand, hourly diversity and pipe condition remain uncertain and require further measurement.

Under the assumptions tested, retaining the existing biomass system is the economically preferred decision. Neither reference heat-pump alternative reaches discounted payback at 115.63 EUR/MWh, while positive capacity-sweep results are limited to 0.50–0.60 MWth at hypothetical prices of 60–69 EUR/MWh and disappear when only half of the estimated avoided O&M is realised. Electricity and biomass prices and genuinely avoidable boiler O&M are therefore the main economic uncertainties. Source-side screening further indicates that COP ≈ 4.4 would require source-water inlet temperatures of approximately 48–53 °C and recoverable heat of 0.77–3.86 MW, depending on heat-pump capacity; no such source has yet been confirmed. Consequently, replacing low-cost hazelnut-shell biomass is difficult to justify financially, while its environmental benefit remains unquantified.

7. References

Averfalk, H., Benakopoulos, T., Best, I., Dammel, F., Engel, C., Geyer, R., Gudmundsson, O., Lygnerud, K., Nord, N., Oltmanns, J., Ponweiser, K., Schmidt, D., Schrammel, H., Østergaard, D.S., Svendsen, S., Tunzi, M., Werner, S., 2021. Low-Temperature District Heating Implementation Guidebook: Final Report of IEA DHC Annex TS2 Implementation of Low-Temperature District Heating Systems (Report No. 978-3-8396-1745–8), Low-Temperature District Heating Implementation Guidebook. Fraunhofer-Verlag.

Averfalk, H., Werner, S., Felsmann, C., Rühling, K., Wiltshire, R., Svendsen, S., 2017. Transformation Roadmap from High to Low Temperature District Heating Systems (Annex XI Final Report). International Energy Agency District Heating and Cooling Programme.

Braas, H., Jordan, U., Best, I., Orozaliev, J., Vajen, K., 2020. District Heating Load Profiles for Domestic Hot Water Preparation with Realistic Simultaneity Using DHWcalc and TRNSYS. Energy 201, 117552. https://doi.org/10.1016/j.energy.2020.117552

Chicherin, S., Mašatin, V., Siirde, A., Volkova, A., 2020. Method for Assessing Heat Loss in a District Heating Network with a Focus on the State of Insulation and Actual Demand for Useful Energy. Energies 13, 4505. https://doi.org/10.3390/en13174505

Comisión Nacional de Energía, 2026. Reporte Financiero del Sector Energético (No. Vol. 36). Comisión Nacional de Energía, Santiago, Chile.

COSSBO, 2024. Operational Logs, Billing Records, Engineering Documents and SCADA Extracts, 2017–2024.

Danish Energy Agency, 2016. Technology Data for Generation of Electricity and District Heating. Danish Energy Agency, Copenhagen, Denmark.

David, A., Mathiesen, B.V., Averfalk, H., Werner, S., Lund, H., 2017. Heat Roadmap Europe: Large-Scale Electric Heat Pumps in District Heating Systems. Energies 10, 578. https://doi.org/10.3390/en10040578

IEA District Heating and Cooling Programme, 2008. District Heating Distribution in Areas with Low Heat Demand Density (Annex VIII Final Report 2008:8DHC-08-03). International Energy Agency District Heating and Cooling Programme.

Jakubek, D., Ocłoń, P., Nowak-Ocłoń, M., Sułowicz, M., Varbanov, P.S., Klemeš, J.J., 2023. Mathematical Modelling and Model Validation of the Heat Losses in District Heating Networks. Energy 267, 126460. https://doi.org/10.1016/j.energy.2022.126460

Kompetenzzentrum Kommunale Wärmewende (KWW), 2024. Leitfaden Wärmeplanung: Technikkatalog. Deutsche Energie-Agentur GmbH (dena).

Lohmeier, D., Cronbach, D., Drauz, S.R., Braun, M., Kneiske, T.M., 2020. Pandapipes: An Open-Source Piping Grid Calculation Package for Multi-Energy Grid Simulations. Sustainability 12, 9899. https://doi.org/10.3390/su12239899

Lund, H., Werner, S., Wiltshire, R., Svendsen, S., Thorsen, J.E., Hvelplund, F., Mathiesen, B.V., 2014. 4th Generation District Heating (4GDH): Integrating Smart Thermal Grids into Future Sustainable Energy Systems. Energy 68, 1–11. https://doi.org/10.1016/j.energy.2014.02.089

QGIS Development Team, 2026. QGIS Geographic Information System.

Ruhnau, O., Hirth, L., Praktiknjo, A., 2019. Time series of heat demand and heat pump efficiency for energy system modeling. Sci Data 6, 189. https://doi.org/10.1038/s41597-019-0199-y

Sayegh, M.A., Jadwiszczak, P., Axcell, B.P., Niemierka, E., Bryś, K., Jouhara, H., 2018. Heat Pump Placement, Connection and Operational Modes in European District Heating. Energy and Buildings 166, 122–144. https://doi.org/10.1016/j.enbuild.2018.02.006

Weissmann, C., Hong, T., Graubner, C.-A., 2017. Analysis of Heating Load Diversity in German Residential Districts and Implications for the Application in District Heating Systems. Energy and Buildings 139, 302–313. https://doi.org/10.1016/j.enbuild.2016.12.096